Iranian Journal of Oil & Gas Science and Technology, Vol. 7 (2018), No. 2, pp. 14-34
http://ijogst.put.ac.ir

A Novel Approach to Measuring Water and Oil Relative Permeabilities in Two-phase Fluid Flow in Porous Media

Azadeh Mamghaderi[1], Behzad Rostami[2*], and Seyed Hamed Tabatabaie[3]

[1]Graduate Student, Institute of Petroleum Engineering, Faculty of Chemical Engineering, College of Engineering, University of Tehran, Tehran, Iran
[2]Associate Professor, Institute of Petroleum Engineering, Faculty of Chemical Engineering, College of Engineering, University of Tehran, Tehran, Iran
[3] Researcher, IHS Global Canada Limited, Alberta, Calgary, Canada

Received: November 25, 2017; *revised*: December 25, 2017; *accepted*: January 10, 2018

Abstract

In this study, direct laboratory measurements of unsteady-state imbibition test are used in a new approach to obtain relative permeability curves with no predetermined functionality assumptions. Four equations of continuity, Darcy's law, cumulative oil production, and water fractional flow are employed in combination together under certain assumptions to present the new approach which interprets these data. We assumed that capillary pressure was previously measured and used as the input data in the method. The main difference between this work and previous unsteady-state methods is to replace the saturation profile, needed to obtain relative permeability curves, with a new saturation-dependent graph which can be measured from recovery data rather than being recorded directly during experiments. The method is demonstrated by employing recovery data from the literature, and it is then verified by a numerical simulator. The results show that the accuracy of the proposed method is comparable with accurate complex methods. Performing sensitivity analysis indicates that the proposed method can achieve more accurate results when applied to cases with a relatively high capillary number and/or low water-oil mobility ratio and when applied to media having uniformly sized pores.

Keywords: Relative Permeability, Waterflooding, Analytical Methods, Saturation Profile, Two-phase Flow

1. Introduction

In describing the fluid flow in oil and gas reservoirs as porous media, relative permeability is a key petrophysical property with a significant effect on the evaluation and forecasting of the reservoir performance (Xu et al., 2013). The relative permeability curves are essential input data in oil and gas reservoir simulators and the accurate determination of their values is of great importance for various types of reservoir studies (Mohamadi-Baghmolaei et al., 2016). Core-scale displacement experiments, including steady-state, unsteady-state, and centrifuge experiments, are performed primarily in order to

* Corresponding Author:
Email: brostami@ut.ac.ir

generate relative permeability curves. The steady-state method is a direct method for obtaining relative permeability from experimental data. This method has the disadvantage of being time-consuming especially for low permeability material (Kamath et al., 1995; Schembre and Kovscek, 2003).

The essence of unsteady-state methods is to estimate relative permeability curves based on measured production (oil and water) histories. Unsteady-state experiments are rapid and relatively easy to perform. The technique of Johnson et al.(1959) and that of Jones and Roszelle (Jones and Roszelle, 1978) are some known unsteady-state methods that neglect capillary pressure based on the Buckley-Leverett theory (Buckley and Leverett, 1942). Simplification assumptions make these methods generally unreliable for low permeability rocks (Akin and Kovscek, 1999). History matching methods are other types of unsteady-state methods that are based on matching experimental data. However, these methods have the disadvantage of being complicated and relatively time consuming. Furthermore, these methods need accurate experimental data, which are not easily obtained, such as a saturation profile and pressure gradient to calculate relative permeability. They need at least an X-ray computerized tomography (CT) scanning method (Schembre and Kovscek, 2006). Table 1 summarizes various available major methods currently being used in the literature to estimate relative permeability.

Table 1
Summary of various available major methods to estimate relative permeability.

Steady-state methods (Christiansen and Howarth, 1995)	• Multiple-core method • High-rate method • Stationary-liquid method • Uniform capillary-pressure method	
Unsteady-state methods (Hussain et al., 2010)	**Analytical methods**	• Johnson-Bossler-Neumann (JBN) method (1959) • Jones and Roszelle (JR) method (1978) • Li et al. method (1994) • Modified JBN method (Kalbus and Christiansen 1995)
	Semi-analytical methods	• Toth et al. method (2002) • Civan and Donaldson Method (1989) • Udegbunam Method (1991)
	History matching	• Power law functional models (Sigmund and McCaffery 1979, McMillan 1987, Grattoni and Bidner 1990) • Spline functions (Kerig and Watson 1986, Subbey et al. 2006, Basbug and Karpyn 2008)

The mentioned unsteady-state methods have been recently challenged because they assume local-equilibrium in porous media during fluid flow modes. Local-equilibrium leads to a self-similar behavior in spontaneous imbibition experiments (Li et al., 2003). In other words, the previous unsteady-state models assume capillary pressure and relative permeability to be solely functions of water saturation that lead to a self-similarity condition. In this regard, based on the theory that the redistribution of two phases in porous media is not instantaneous when the media is filled by water, some recent studies consider non-equilibrium effects on reservoir recovery and its properties (Schembre and Kovscek, 2006; Barenblatt et al., 2003; Silin and Patzek, 2004; Le Guen and Kovscek, 2006). Mainly focused on counter-current spontaneous imbibition, these studies attempted to show that capillary pressure and relative permeability are not solely functions of instantaneous water

saturation. Schembre and Kovscek (Schembre and Kovscek, 2006) provided a methodology to involve non-equilibrium effects in the interpretation of unsteady-state laboratory data in order to obtain steady-state relative permeability curves. Saturation profiles in their method are measured as a function of time by X-ray CT during the experiments.

Empirical correlations and analytical mathematical models (Purcell, 1949; Corey, 1954; Honarpour et al., 1982; Ibrahim and Koederitz, 2000; Lomeland et al., 2005; Mosavat et al., 2013; Xu et al., 2015) are used for forecasting relative permeability curves in two different ways: first, predicting relative permeability as a function of some media properties such as capillary pressure, absolute permeability, porosity, fluid saturation etc.; second, defining relative permeability as a parametric model in which required parameters are obtained by implementing measured experimental data (Mohamadi-Baghmolaei et al., 2016).

In this work, we introduce an analytical approach which uses laboratory measured data as input data in an effective way to predict water and oil relative permeability curves in imbibition experiments. As mentioned earlier, taking into account the non-equilibrium effects leads to the need of recording saturation profile history as a function of time. However, our new approach uses input data to obtain a saturation-distance graph which does not change with time; therefore, there is no need to monitor the saturation distribution in the laboratory that may be time consuming and costly. This approach makes the experiment a fast way to estimate imbibition relative permeability curves, at least for non-tight cores. Considering the relative permeability of a media property that may be affected by non-equilibrium effects, the saturation parameter itself is set to be time-dependent in our approach, which leads to the inclusion of time effects in the interpretation. We first present the mathematical derivation of the new approach and evaluate it by related experimental data extracted from open literature. Here, any approximations and assumptions of the method are discussed. Then, we investigate the method's applicability range, and ten synthetic cases are modeled by a numerical simulator to define the effects of various involved variables on the accuracy of the proposed method.

2. Mathematical derivation

We describe a new method that can be used to calculate water and oil relative permeabilities for waterflooding test. The four using fundamental equations are: (i) a continuity equation for a 1-D fluid flow procedure in porous media, (ii) an extended form of Darcy's law for two-phase fluid flow, (iii) the cumulative oil production equation, and (iv) a water fractional flow equation for a system producing water and oil simultaneously.

In a coreflooding process, a wetting phase displaces a non-wetting phase, and this leads to the same movement direction of the two phases. We relate the inlet and outlet rates through the media by the continuity equation then combine it with the extended form of Darcy's law for two-phase fluid flow:

$$\frac{q_{inj}}{A}(S_{wL}-S_{wi})\left.\frac{\partial f_w}{\partial S_w}\right|_{S_{wL}} = -\frac{k.k_{rw}}{\mu_w}\left.\frac{\partial p_w}{\partial x}\right|_{S_{wL}} \tag{1}$$

To calculate water saturation at the end of the core, S_{wL}, we call the cumulative oil production equation:

$$N_p = \int_0^t q_o dt \tag{2}$$

Considering $q_o = (1 - f_w) q_{inj}$, assuming that q_{inj} is constant, and then taking integration from the above equation leads to:

$$N_p = q_{inj} \left[t(1 - f_w) + \int_0^R t.df_w \right] \tag{3}$$

Recalling the continuity equation while neglecting fluid compressibility with the assumption that x is not a function of $\frac{df_w}{dS_w}$ and taking integration from that, we have:

$$x = \frac{q_{inj} t}{A.\phi} \frac{df_w}{dS_w} \tag{4}$$

We rearrange the above equation for the end of the core, where x is replaced by core length, L, and then combine it with Equation 3:

$$N_p = q_{inj}. \left[t(1 - f_w) + \int_{S_{wi}}^{S_{wL}} t. \frac{A.\phi.L}{q_{inj} t} dS_w \right] \tag{5}$$

By taking integration from the second term of Equation 5 and then rearranging the resulting equation, S_{wL} can be calculated as:

$$S_{wL} = S_{wi} + \frac{N_p - q_{inj} t(1 - f_w)}{A.\phi.L} \tag{6}$$

where, water fractional flow, f_w, can be obtained from production data:

$$f_w = \frac{q_w}{q_w + q_o} \tag{7}$$

Thus, water saturation at the end of the core can be measured at any time. This time-dependent parameter plays a critical role in the calculation of relative permeabilities in our approach. Water does not appear before the breakthrough time; therefore, t in Equation 6 starts from the breakthrough time and is followed by the after-breakthrough times. Using $P_c = p_o - p_w$ and assuming that the pressure gradient in the oil phase is negligible lead to rearranging Equation 1 as:

$$k_{rw} = \frac{q_{inj}.\mu_w}{A.k} \left. \frac{\partial f_w}{\partial S_w} \right|_{S_{wL}} (S_{wL} - S_{wi}) \frac{1}{(\partial P_c / \partial x)_{S_{wL}}} \tag{8}$$

Considering that P_c is a function of S_w only, the water relative permeability is then obtained from:

$$k_{rw} = \frac{q_{inj}.\mu_w}{A.k} \left. \frac{\partial f_w}{\partial S_w} \right|_{S_{wL}} \left(S_{wL} - S_{wi} \right) \frac{1}{\left(\frac{dP_c}{dS_w} \frac{dS_w}{dx} \right)_{S_{wL}}} \tag{9}$$

This equation suggests that water relative permeability can be calculated by finding the three derivative terms in this equation, including $\frac{\partial f_w}{\partial S_{wL}}$, $\frac{dP_c}{dS_{wL}}$, and $\frac{dS_{wL}}{dx}$. Because the after-breakthrough times are used to calculate S_{wL}, we use the breakthrough time to calculate each x term related to each water saturation term at the end of the core:

$$x' = \frac{q_{inj} t_{B.T}}{A.\phi} \left. \frac{\partial f_w}{\partial S_w} \right|_{S_{wL}} \tag{10}$$

We assume that $\frac{dS_{wL}}{dx}$ is approximated by:

$$\frac{dS_{wL}}{dx} = \left(\frac{dS_w}{d \ln x'} \right)_{x=L} \frac{1}{L} \tag{11}$$

in which, S_{wL} is time-dependent, but the graph of S_{wL} versus $\ln x'$ does not change with time. When we replace it in Equation 9:

$$k_{rw} = \frac{q_{inj.}\mu_w}{A.k} \left. \frac{\partial f_w}{\partial S_w} \right|_{S_{wL}} (S_{wL} - S_{wi}) \frac{L}{\left(\frac{dP_c}{dS_w} \frac{dS_w}{d \ln x'} \right)_{x=L}} \tag{12}$$

Applying the general expression for water fractional flow in a horizontal system of water-oil:

$$f_w = \frac{1 + \frac{k.k_{ro}.A}{q_{inj}.\mu_o} \left(\frac{\partial P_c}{\partial x} \right)}{1 + \frac{k_{ro}}{k_{rw}} . \frac{\mu_w}{\mu_o}} \tag{13}$$

and then rearranging the above equation under the same assumptions for k_{rw}, k_{ro} can be obtained as:

$$k_{ro} = \frac{1 - f_w}{\frac{f_w}{k_{rw}} . \frac{\mu_w}{\mu_o} - \frac{k.A}{q_{inj}.\mu_o.L} \left(\frac{dP_c}{dS_w} \frac{dS_w}{d \ln x'} \right)_{x=L}} \tag{14}$$

3. Application of the method

We use recovery data of an experimental work by Qadeer et al. (2002) to demonstrate the application of the new method. These data were obtained from waterflooding into Berea Quarry sandstone, a material known as relatively high permeability (720 md) media which is also homogeneous and strongly water wet with relatively uniform properties. The average porosity of the samples was 0.2. The total designed experiments by Qadeer et al. are presented in Table 2.

Table 2
Sequence of displacement experiments by Qadeer et al., 2002.

Displacement	Flow Rate (cc/min)
Primary drainage	8.59
Imbibition-1	8.43
Drainage-1	8.60
Imbibition-2	3.77
Drainage-2	4.28
Imbibition-3	1.04
Drainage-3	1.07

We only use the Imbibition-3 experimental data in this study due to the fact that there is little recovery after the breakthrough time in the other imbibition tests. The experiments were conducted using 8% sodium bromide as the wetting phase (with initial saturation of 0.46) and cyclohexane as the non-wetting phase. The measured imbibition capillary pressure curve by the centrifuge method for similar Berea sandstone cores (Qadeer, 1988) was used as shown in Figure 1(a).

Qadeer et al. used CT imaging to measure the saturations during their displacement experiments. They obtained relative permeability curves based on the automated history matching procedure of Levenberg-Marquardt as described by Press et al. (1990).

The measured recovery data by Qadeer et al. are presented in Figure 1(b) for the Imbibition-3 test.

All parameters needed to estimate water and oil relative permeabilities using our approach are provided by these experimental data. Recovery data, Figure 1(b), is used to calculate f_w, t, and N_p. An area of 20.258 cm^2 and a length of 25.4 cm are used for A and L respectively. Water saturation at the end of the core is, therefore, calculated by Equation 6 for all recorded time data. Breakthrough time is obtained from Figure 1(b), where oil recovery is changed immediately; then, x' can be calculated by using Equation 10. The capillary pressure curve, Figure 1(a), is used to calculate $\frac{dP_c}{dS_{wL}}$. The resulting k_{rw} and k_{ro}, respectively defined by Equations 12 and 14, are compared with the history matching results by Qadeer et al. as displayed in Figure 1(c). As shown in this figure, good agreement is obtained between the two methods.

a)

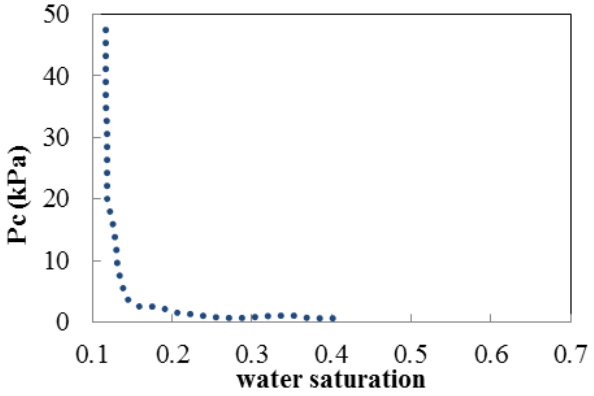

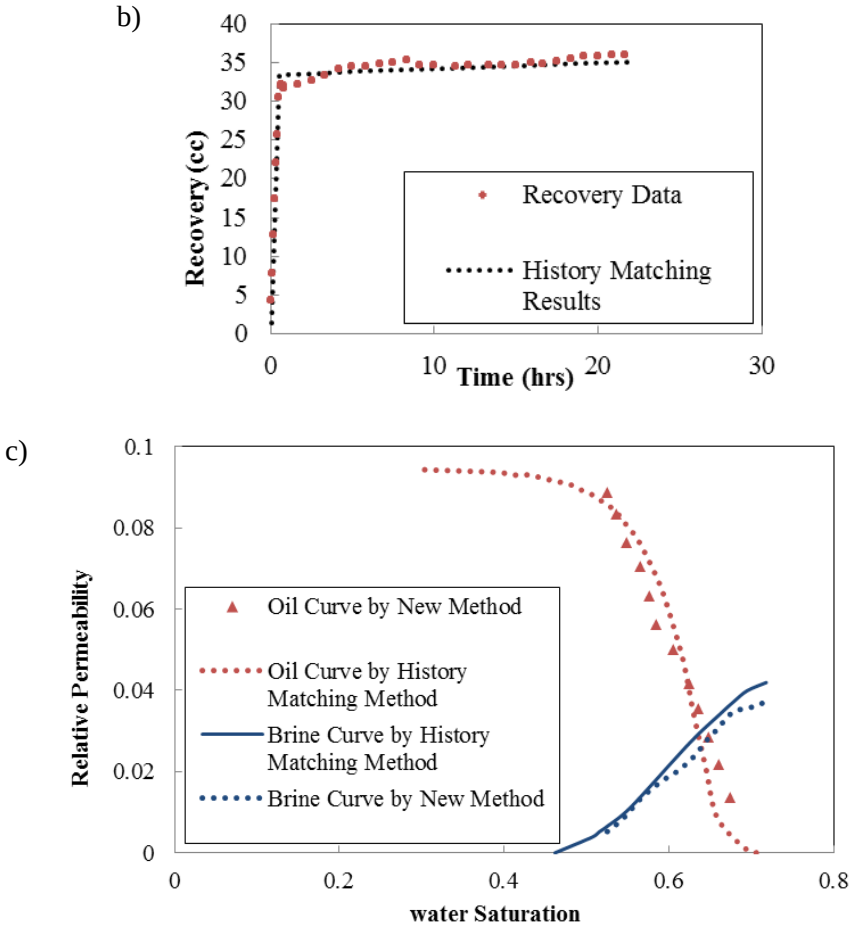

Figure 1
a) Capillary pressure curve by the centrifuge method for Berea sandstone cores (Qadeer, 1988); b) Recovery match for the Imbibition-3 test by Qadeer et al. (2002); c) Comparison of relative permeability curves for Imbibition-3 test obtained by HM (Qadeer et al., 2002) and the new approach.

4. Approximations

The new estimation method in this study makes several approximations. First, the method is appropriate for experiments in which recovery is considerable after the breakthrough time because t starts from the breakthrough time in Equation 6. Second, we suppose that capillary pressure is previously estimated by another procedure and use it directly in our new method; this makes the method dependent on the input capillary pressure. After fixing the capillary pressure, however, there is no need to use and fix parametric equations to define a unique solution for relative permeability curves. This means that we do not need pre-figuration of the relative permeability curves. Third, we neglect the pressure gradient in the oil phase in our derivation of relative permeabilities. Generally, this makes our method especially suitable for water/gas flows or for water into light hydrocarbons. This assumption was previously used by other methods in the literature (Hughes and Blunt, 2001; Schembre and Kovscek, 2003). Although the oil phase pressure gradient is neglected when finding water relative permeability, the method also yields non-wetting phase relative permeability according to Equation 14. Fourth, instead of any recorded water saturation distribution in the core, we assume that the slope of the graph of water saturation at the end of the core versus x, approximated by Equation 11, is used in our calculations. This assumption can be true because the trend (slope) of water saturation distribution versus the position of the fluid front, S_w versus x, at the breakthrough

time is regenerated by S_{wL} versus x'. Figure 2 shows the similar trends of these two curves for the experimental data of Qadeer et al. (2002) at an injection rate of 1.04 cc/min. Fifth, due to the fact that we assumed unique porosity and permeability in the derivations of the method's equations, the recovery data are obtained for a homogeneous media. Finally, because capillary end effects emerge due to the discontinuity of capillarity in the wetting phase at the outlet of the core and this effect is prominent in drainage process where the wetting phase is being displaced by non-wetting phase (Huang and Honarpour, 1998), we neglect this effect for the derivation of relative permeability in our imbibition tests.

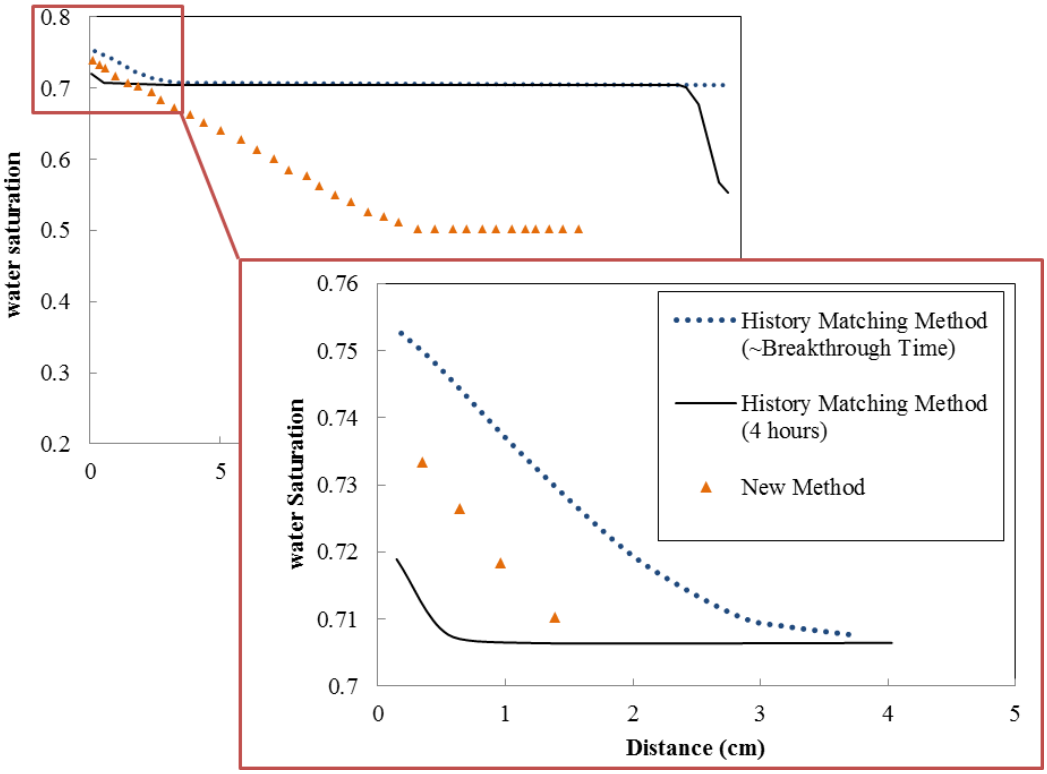

Figure 2
Water saturation profile for the Imbibition-3 test.

Besides the assumptions made above, it should be mentioned that we consider the relative permeability a property that may be affected by non-equilibrium effects in our approach where we used a time-dependent saturation parameter. In (Mirzaei-Paiaman et al., 2011) various contradictory claims about the existence and contribution of non-equilibrium effects to multi-phase flow models was investigated, and the results show that non-equilibrium effects exist in all imbibition modes (co-current and counter-current imbibition). They stated that non-equilibrium effects exist during the spontaneous imbibition process but their effect may not be significant enough to affect oil recovery versus time, while water saturation versus the similarity variable for different times will be affected.

All these approximations in combination together allow the model to successfully predict water and oil relative permeability curves in two-phase fluid flow.

5. Verification of the method

The applicability of the new method in determining relative permeability curves is examined by analyzing the effects of changing some included parameters on the accuracy of the developed

approach. We use a 1-D numerical simulator in order to design appropriate cases to study these effects.

5.1. Simulated example

A 1-D numerical simulator is used to show the efficiency of our derivations. The descriptions and details of the simulator are presented in Appendix. In order to show the application of the data generated by the simulator in our proposed method, we apply an imbibition experiment as given by Schembre and Kovscek (Schembre and Kovscek, 2003). This experiment is simulated in the numerical simulator; then, its resulted recovery data are applied to the new method. Schembre and Kovscek used an X-ray CT method to obtain saturation profiles along the cores. In their method, a previously measured capillary pressure curve was used as the input data. n-decane was the non-wetting fluid, and the initial water saturation was zero. The properties of the porous media and the fluid data are presented in Table 3. The input capillary pressure and the relative permeability curves of their method are also used as the input data to the numerical simulator. These curves are shown in Figure 3(a) and Figure 3(b) respectively.

Table 3
Characteristics of the porous media and the fluid data of the case study (Schembre and Kovscek, 2003).

Item	Value
Permeability, k (md)	6.6
Porosity, ϕ (fraction)	0.65
Length, L (cm)	8.8
Compressibility, c (kPa^{-1})	7.25×10^{-6}
Brine density, ρ_w (g/cc)	1.0
Oil density, ρ_o (g/cc)	0.8
Brine viscosity, μ_w (cP)	1.0
Oil viscosity, μ_o (cP)	0.86

a)

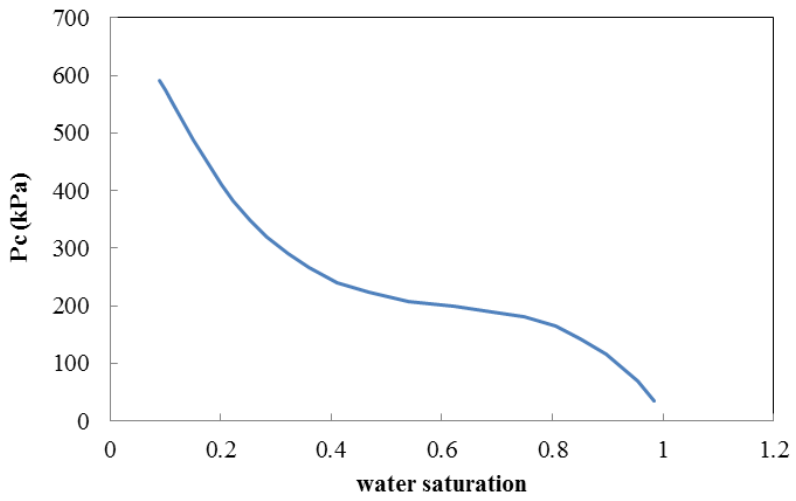

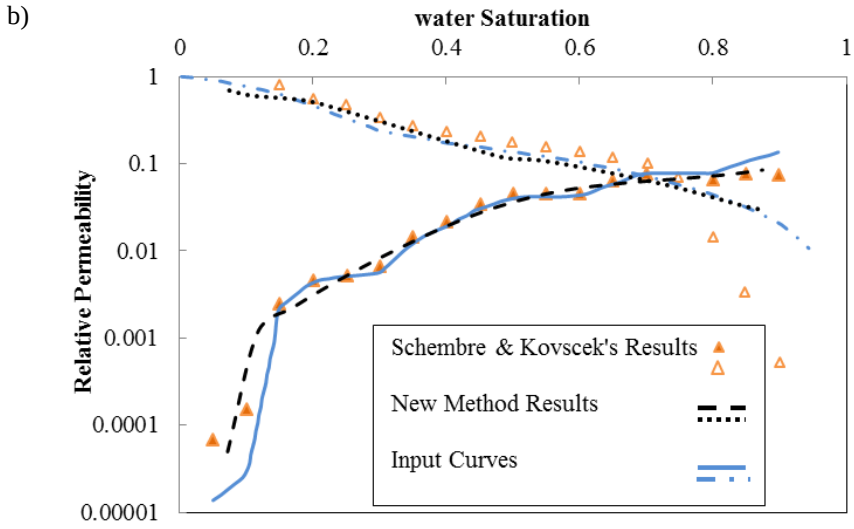

Figure 3
a) Input capillary pressure curves for Schembre and Kovscek's work (Schembre and Kovscek, 2003); b) The new approach results in comparison with the input curves and Schembre and Kovscek's (Schembre and Kovscek, 2003) relative permeability curves.

The resulting recovery data from the simulator is used in our new proposed method to calculate water and oil relative permeabilities by Equations 12 and 14 respectively. Figure 3(b) presents input relative permeability curves, the curves obtained by our proposed method and the ones obtained by Schembre and Kovscek in comparison with each other. Like the results of Schembre and Kovscek's method, the results of our approach are well matched with the input curves in an acceptable range of water saturation.

5.2. Sensitivity analysis

We vary some involved variables in the proposed method, including the water injection rate, threshold pressure, oil viscosity, input capillary pressure, and input relative permeability curves to study the applicability of the new approach in various displacement experimental designs. As the base case, a 1-D porous media with an absolute permeability of 100 md and a length of 60 cm is considered. The input relative permeability and imbibition capillary pressure functions are assumed to be expressed by Brooks-Corey correlations (Brooks and Corey, 1966):

$$k_{rw} = k_{rw}^{0}(S_w^*)^{3+2/\lambda}, k_{ro} = k_{ro}^{0}(1-S_w^*)^{3+2/\lambda} \tag{15}$$

$$P_c = P_{th}(S_w^*)^{-1/\lambda} \tag{16}$$

where, λ is the Brooks-Corey pore size distribution index, and S_w^* is the normalized water saturation expressed by:

$$S_w^* = \frac{S_w - S_{wr}}{1 - S_{wr} - S_{or}} \tag{17}$$

Table 4 tabulates the properties used for the porous media and the fluids in the base case example. The input data are used to build the base case that is modeled by the numerical simulator; then, its resulted recovery data are applied directly to the new method to regenerate the input (true) curves of

relative permeabilities, independent of them. Good matched results are obtained by the comparison of the input and resulting relative permeability curves as shown in Figure 4.

Table 4
Base case media and fluid properties.

Item	Value
Absolute Permeability, k (md)	100
Area, A (cm^2)	9
Length, L (cm)	60
Porosity, ϕ (fraction)	0.4
Oil viscosity, μ_o (cP)	0.5
Water viscosity, μ_w (cP)	1
Entry Pressure, P_{th} (kPa)	20
k_{rw}^0	1
k_{ro}^0	1
λ	4
Water injection rate, q_{inj} (cc/min)	0.006

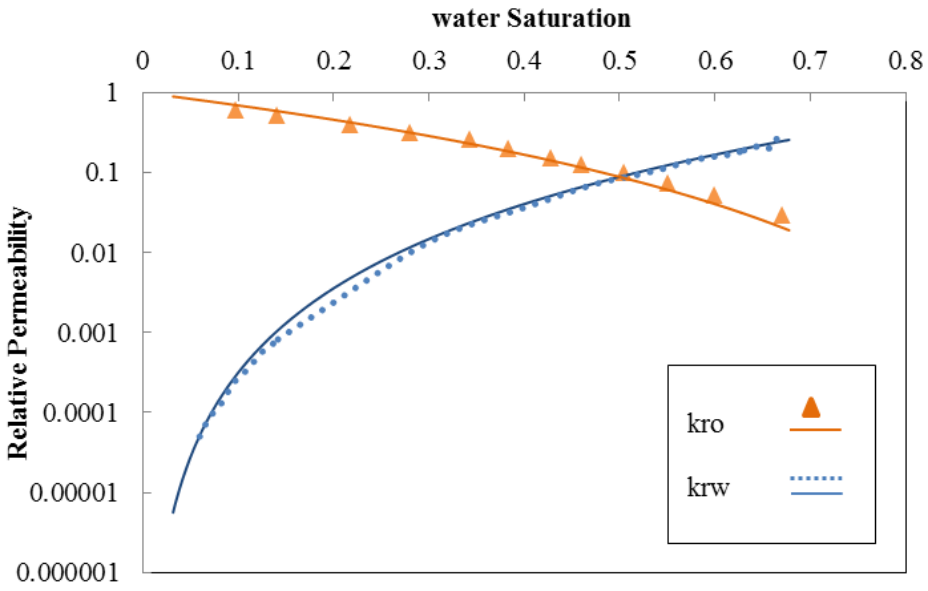

Figure 4
Comparison between the input curve (solid line) and the proposed method's result for the base case.

We designed nine different cases to cover different ranges of involved parameters. As with the base case, by applying the numerical simulator and using its resulting recovery data as the inputs to the new proposed method, water and oil relative permeabilities are calculated. Then, in comparison with the input relative permeabilities, the accuracy of the new method is indicated. A list of the designed cases is tabulated in Table 5. The parameter studied in this table presents the change of the case against the base case.

Table 5
List of cases studied in the estimation of water and oil relative permeabilities.

Case ID	Parameter studied	Value
1	**Water injection rate**	0.003 cc/min
2	**Water injection rate**	0.008 cc/min
3	**Water injection rate**	0.01 cc/min
4	**Threshold pressure**	10 kPa
5	**Threshold pressure**	30 kPa
6	**Oil viscosity**	1 cP
7	**Oil viscosity**	3 cP
8	λ	2
9	λ	∞

a. Injection rate

Cases 1–3 in Table 5 are designed to study the effect of water injection rate on the accuracy of the new proposed method as shown in Figure 5(a).

It is revealed from this figure that by increasing the injection rate the accuracy of the approach increases. This can be described by considering the changes in the Capillary Number (N_c) as a result of changes in the flow rate. N_c is usually large for high-speed flows and low for low-speed flows; thus, it is expected to increase as a result of increasing the injection rate:

$$N_c = \frac{q\mu}{\sigma} \tag{18}$$

Oil is connected from the inlet to the outlet at any time during the displacement processes in the case of low N_c and during the commencement of the displacement processes in the case of intermediate to high N_c. Progressing displacement in the latter leads to decreasing oil saturation, and the oil connected region start-point, known as the oil sub-network, progressively moves towards the outlet (Idowu and Blunt, 2009). Since no pressure drop occurs outside the oil sub-network, and we assume negligible oil pressure gradient in the proposed method, it is expected that the results show improved accuracy when the oil sub-network moves faster in the region. The assumption for a much longer time during the displacement process seems more desirable. We confirm the effect of N_c by changing the threshold pressure, P_{th}, in cases 4–5 as presented in Table 5. For a cylindrical throat of radius r with no contact angle hysteresis, we have:

$$P_{th} = \frac{2\sigma\cos\theta_r}{r} \tag{19}$$

where, P_{th} is in direct relation with interfacial tension, σ. Assuming no changes in the pore's radius, r, and contact angle, θ_r, an increase in σ leads to an increase in P_{th} and a decrease in N_c. Considering the results in Figure 5(b) and the base case plot shows improved accuracy for the cases having smaller P_{th}'s.

b. Oil viscosity

The effect of changing oil viscosity is studied in cases 6–7 as shown in Figure 5(c). It is clear that by increasing oil viscosity and having it approach water viscosity the method makes no changes in the accuracy of the results. Then, by increasing oil viscosity to a value higher than that of water viscosity, the results show some errors. This refers to the approximation that makes the method accurately describe displacement processes for gases and relatively light hydrocarbons. It can be inferred from this analysis that cases with a lower water-oil mobility ratio can be better described by the approach.

c. Properties of the porous media

Since we consider Corey-type correlations to describe input relative permeability and capillary pressure curves for the numerical simulator, we can study the effects of these properties on the applicability of the new proposed method by changing λ in Equations 15 and 16. The related designed cases are cases 8–9 in Table 5. The results are shown in Figures 5(d) through 5(e) and show that by increasing λ from 2 to ∞ the accuracy of the method increases. Brooks and Corey (Brooks and Corey, 1966) stated that the values of 2, 4, and ∞ express the situations of a wide range of pore size, a medium range of pore size, and a single uniform pore size respectively. In reality, we are changing the porous media heterogeneity by changing λ. By increasing λ from 2 to ∞ to decrease the heterogeneity of the porous media, the accuracy of the method increases. However, due to the fact that we made some approximations regarding media heterogeneity in our numerical simulator, like assuming unique porosity and permeability, the recovery data are obtained for a homogeneous media. Applying these data to the proposed method may also affect the errors related to heterogeneity.

a)

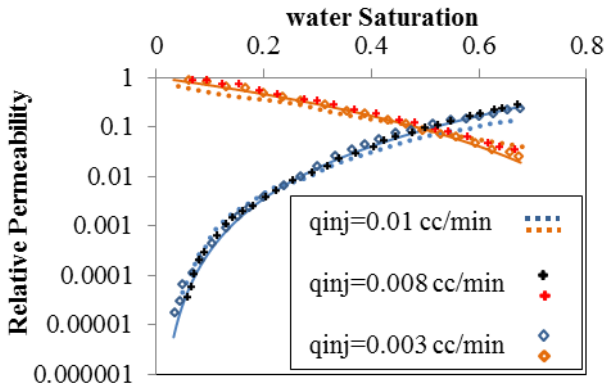

b)

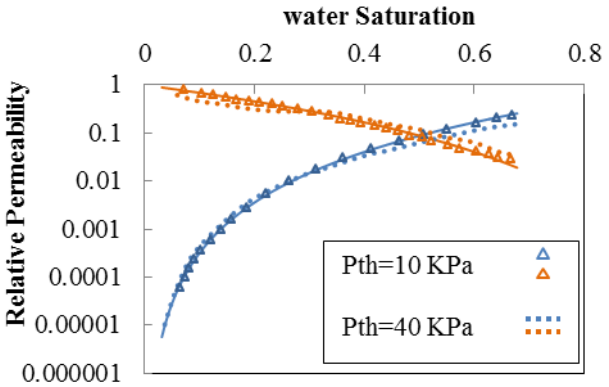

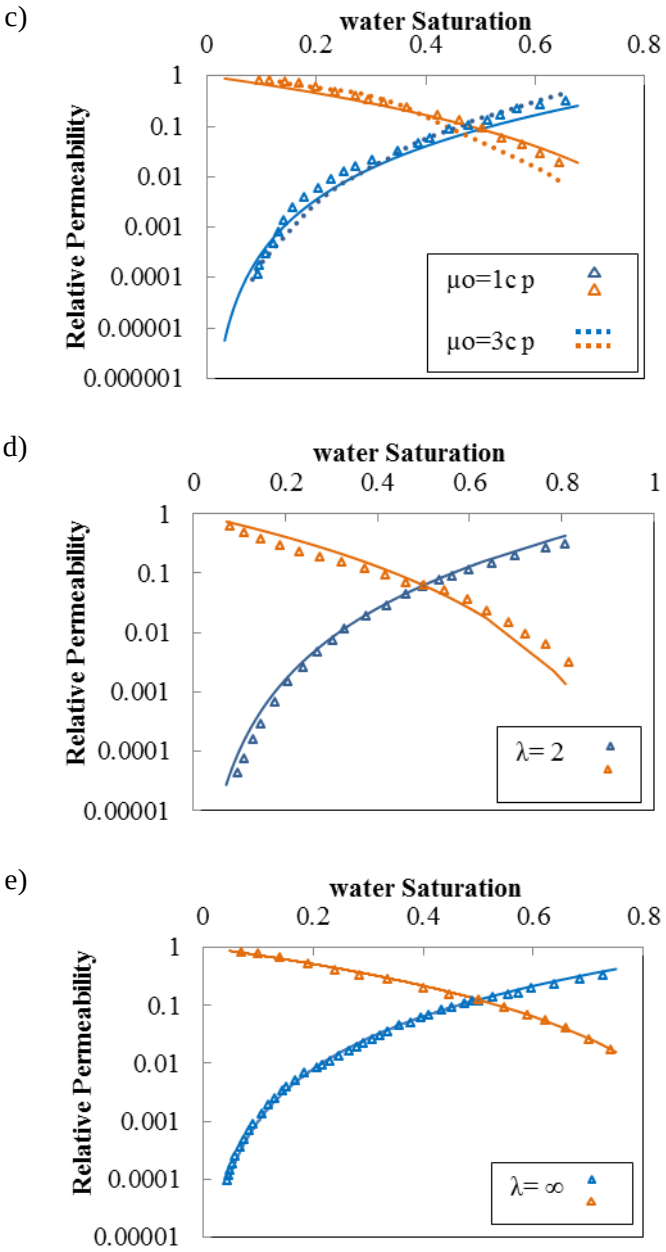

Figure 5
a) Comparison between the input curve (solid line) and the proposed method result for cases 1–3; b) Comparison between the input curve (solid line) and the proposed method result for cases 4–5; c) Comparison between the input curve (solid line) and the proposed method result for cases 6–7; d) Comparison between the input curve (solid line) and the proposed method result for case 8; e) Comparison between the input curve (solid line) and the proposed method result for case 9.

6. Conclusions

A saturation profile should be recorded as a function of time through unsteady-state experiments in order to be used in multiphase flow properties assessment, especially in the new methods, which have been introduced in the last decade and take into account non-equilibrium effects. A new interpretation method for the recovery data from laboratory experiments of waterflooding processes was introduced providing a saturation-distance graph that does not change with time and can be used instead of the common saturation distribution profile to obtain relative permeability curves. The inclusion of time in

the saturation calculation in this method may be considered a way to capture the time effects in the interpretation. The experimental data from the literature was used to validate the method. The comparison of the developed model with other accepted methods revealed a good match between the results. The effects of capillary number, oil viscosity, and the heterogeneity of the porous media on the applicability of the method were investigated by a numerical simulator, and the following results were obtained.

1- A relatively high capillary number yields very good matched results.
2- Due to the method approximations, better results were achieved for cases with a relatively low water-oil mobility ratio.
3- The results of the method for the porous media with a uniform pore size show higher accuracy than the results of the method for the porous media with a wider range of pore sizes.

Acknowledgments

The authors are deeply grateful to Prof. Mehran Pooladi-Darvish for his valuable suggestions and recommendations that were essential in the derivation of the analytical formulations at every stage of this research.

Nomenclature

A	: Cross sectional area
K	: Absolute permeability
k_r	: Relative permeability
k_r^0	: End point relative permeability at residual saturation
L	: Length of core
P	: Pressure
P_{cow}	: Capillary pressure
P_{th}	: Threshold pressure
Q	: Rate
R	: Production time
S	: Saturation
S_r	: Residual saturation
Greek Letters	
ϕ	: Porosity
μ	: Viscosity

References

Akin, S. and Kovscek, A. R., Imbibition Studies of Low-permeability Porous Media, Presented at the Proceedings of the SPE Western Regional Meeting, Anchorage Alaska, USA, 1999.

Barenblatt, G. I., Silin, D. B., and Patzek, T. W., The Mathematical Model of Non-equilibrium Effects in Water-oil Displacement, SPE Journal, Vol. 8, p. 409-416, 2003.

Brooks, R. H. and Corey, A. T., Properties of Porous Media Affecting Fluid Flow, Journal of Irrigation and Drainage Engineering, Vol.6, No.61, 1966.

Buckley, S. E. and Leverett, M. C., Mechanism of Fluid Displacement in Sands, Transactions of the AIME ,Vol. 146, p. 107-116, 1942.

Christiansen, R, L. and Howarth, S, M., Literature Review and Recommendation of Methods for Measuring Relative Permeability of Anhydrite from the Salado Formation at the Waste Isolation Pilot Plant, Sandia National Laboratories, United States Department of Energy, 1995.

Corey, A.T., the Interrelation between Gas and Oil Relative Permeabilities, Producers Monthly, Vol. 19, p. 38–41, 1954.

Honarpour, M., Koederitz, L., and Harvey, A. H., Empirical Equations for Estimating Two Phase Relative Permeability in Consolidated Rock, Journal of Petroleum Technology, Vol. 34, p. 2905–2908, 1982.

Huang, D, D. and Honarpour, M, M., Capillary End Effects in Core Flood Calculations,Journal of Petroleum Science and Engineering, Vol. 19, p. 103-117, 1998.

Hughes, R. G. and Blunt, M. J., Network Modeling of Multiphase Flow in Fractures, Advances in Water Resour., Vol. 24, p. 409-421, 2001.

Hussain, F., Cinar, Y., and Bedrikovetsky, P., Comparison of Methods for Drainage Relative Permeability Estimation From Displacement Tests, SPE Improved Oil Recovery Symposium held in Tulsa, Oklahoma, USA, 24–28 April, 2010.

Ibrahim M. and Koederitz, L., Two-phase Relative Permeability Prediction Using a Linear Regression Model, SPE Eastern Regional Meeting, Society of Petroleum Engineers, 2000.

Idowu, N. A. and Blunt, M. J., Pore-scale Modelling of Rate Effects in Waterflooding, Transport in Porous Media, Vol. 83, p. 151-169, 2009.

Johnson, E. E., Bossler, D. R., and Naumann, V. O., Calculation of Relative Permeability from Displacement Experiments, Transactions of the AIME, Vol. 216, p. 370-372, 1959.

Jones, C. C. and Roszelle, W. O., Graphical Techniques for Determining Relative Permeability from Displacement Experiments, Journal of Petroleum Technology, Vol. 30, p. 807-817, 1978.

Kamath, J., deZabala, E.F., and Boyer, R.E., Water/oil Relative Permeability Endpoints of Intermediate-wet, Low Permeability Rocks, SPE Formation Evaluation, Vol. 10, No. 1, p. 4-10, 1995.

Le Guen, S. S. and Kovscek, A. R., Non-equilibrium Effects during Spontaneous Imbibitions, Transport in Porous Media., Vol. 63, p. 127-146, 2006.

Li, Y., Morrow, N. R., and Ruthb, D., Similarity Solution for Linear Countercurrent Spontaneous Imbibitions, Journal of Petroleum Science and Engineering, Vol. 39, p. 309-326, 2003.

Lomeland, F., Ebeltoft, E., and Thomas, W.H., A New Versatile Relative Permeability Correlation, International Symposium of the Society of Core Analysts, Toronto, Canada, , p.1-12, 2005.

Mirzaei-Paiaman, A., Masihi, M., and Standnes, D. C., Study on Non-equilibrium Effects during Spontaneous Imbibition, Energy Fuels, Vol 25, No.7, p. 3053–3059, 2011.

Mohamadi-Baghmolaei, M., Azin, R., Sakhaei, Z., Mohamadi-Baghmolaei, R., and Osfouri, S., Novel Method for Estimation of Gas/Oil Relative Permeabilities, Journal of Molecular Liquids, Vol. 223, p. 1185-1191, 2016.

Mosavat, N., Torabi, F., and Zarivnyy, O., Developing New Corey-based Water/Oil Relative Permeability Correlations for Heavy Oil Systems, SPE Heavy Oil Conference-Canada, Society of Petroleum Engineers, 2013.

Press, W. H., Teukolsky, S. A., Vetterling, W. T., and Flannery, B. P., Numerical Recipes in FORTRAN, Cambridge University Press, 1990.

Purcell, W., Capillary Pressures Measurement Using Mercury and the Calculation of Permeability Therefrom, Journal of Petroleum Technology, Vol. 1, p. 39–48, 1949.

Qadeer, S., Correcting Oil-water Relative Permeability Data for Capillary End Effects, Master of Science Thesis, University of Alaska, Fairbanks, Alaska, 1988.

Qadeer, S., Brigham, W. E., and Castanier, L. M., Techniques to Handle Limitations in Dynamic Relative Permeability Measurements, U.S. Department of Energy Assistant Secretary for Fossil Energy, 2002.

Schembre, J. M. and Kovscek, A. R., A Technique for Measuring Two-phase Relative Permeability in Porous Media via X-ray CT Measurements, Journal of Petroleum Science and Engineering, Vol. 39, p. 159-174, 2003.

Schembre, J. M. and Kovscek, A. R., Estimation of Dynamic Relative Permeability and Capillary Pressure from Countercurrent Imbibition Experiments, Transport in Porous Media, Vol. 65, p. 31-51, 2006.

Silin, D. B. and Patzek, T. W., On the Barenblatt Model of Non-equilibrium Imbibitions, Transport in Porous Media., Vol. 54, p. 297-322, 2004.

Xu, P., Qiu, S., Yu, B., and Jiang, Z., Prediction of Relative Permeability in Unsaturated Porous Media With a Fractal Approach, International Journal of Heat and Mass Transfer, Vol. 64, p. 829-837, 2013.

Xu, J., Guo, C., Jiang, R., and Wei, M., Study on Relative Permeability Characteristics Affected by Displacement Pressure Gradient: Experimental Study and Numerical Simulation, Fuel, Vol. 163, p. 314–323, 2015.

Appendix: Numerical Simulator

Two-phase simulation model

In the following, we derive equations for two-phase flow models. The flow equations are obtained first by discretizing the core into grid blocks as shown in Figure A, followed by writing the material balance of the components for block *i* and combining it with the Darcy's Law. Figure A shows a block-centered grid for a 1-D core in the direction of *x* axis. The grid is constructed by choosing *n x* grid blocks that span the entire core length in the *x* direction.

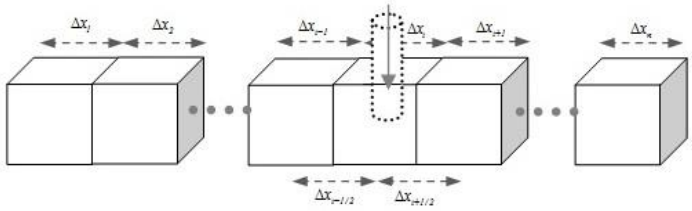

Figure A

Discretization of a 1-D core using a block-centered grid model.

For block *i* in Figure A, the mass balance equation for component *s* can be written as:

$$\int_{t^n}^{t^{n+1}} \omega_{sx}\big|_{x_{i-1/2}}\, dt - \int_{t^n}^{t^{n+1}} \omega_{sx}\big|_{x_{i+1/2}}\, dt + \int_{t^n}^{t^{n+1}} q_{sm_i}\, dt = V_{b_i}\,(m_{sv_i}^{n+1} - m_{sv_i}^{n}) \tag{A}$$

The fluid volumetric velocity (flow rate per unit cross-sectional area) of phase *s* from block *i*-1 to *i* is given by Darcy's Law:

$$u_{sx}\big|_{x_{i-1/2}} = \beta_c \frac{(k_x k_{rs})\big|_{x_{i-1/2}}}{\mu_s\big|_{x_{i-1/2}}} \left[\frac{\phi_{s_{i-1}} - \phi_{s_i}}{\Delta x_{i-1/2}} \right] \tag{B}$$

In which, the potential difference between block *i*-1 and block *i* is defined as:

$$\phi_{s_{i-1}} - \phi_{s_i} = (p_{s_{i-1}} - p_{s_i}) - \gamma_{s_{i-1/2}} (Z_{i-1} - Z_i) \tag{C}$$

By combining Equation B with the mass balance equation, we obtain:

$$\begin{aligned} &\int_{t^n}^{t^{n+1}} \{T_{sx_{i-1/2}} [(p_{s_{i-1}} - p_{s_i}) - \gamma_{s_{i-1/2}} (Z_{i-1} - Z_i)]\} dt + \int_{t^n}^{t^{n+1}} \{T_{sx_{i+1/2}} [(p_{s_{i+1}} - p_{s_i}) - \gamma_{s_{i+1/2}} (Z_{i+1} - Z_i)]\} dt \\ &+ \int_{t^n}^{t^{n+1}} q_{ssc_i}\, dt = \frac{V_{b_i}}{\alpha_c} [(\frac{\phi S_s}{B_s})_i^{n+1} - (\frac{\phi S_s}{B_s})_i^{n}] \end{aligned} \tag{D}$$

where, transmissibility is defined as:

$$T_{sx_{i\pm1/2}} = (\beta_c \frac{k_x A_x k_{rs}}{\mu_s B_s \Delta x})\Big|_{x_{i\pm1/2}} \tag{E}$$

The derivation of the Equation D is rigorous and involves no assumptions other than the validity of Darcy's Law for multiphase flow to estimate the *s*-phase volumetric velocities between block *i* and its neighboring blocks *i*-1 and *i*+1. The inter-block geometric factor between block *i* and its neighboring blocks $\left(\beta_c \frac{k_x A_x}{\Delta x}\Big|_{x_{i\pm1/2}} \right)$ is constant, independent of space and time. The relative permeability of the water phase between block *i* and neighboring blocks at any instant of time *t* ($k_{rs}|_{x_{i\pm1/2}}$) uses the upstream value or two point upstream value of block *i* and neighboring blocks that are already fixed in space. In other words, the term $k_{rs}|_{x_{i\pm1/2}}$ is not a function of space but a function of time as the block saturation change with time. Hence, transmissibility $T_{sx_{i\pm1/2}}$ between block *i* and neighboring blocks is a function of time only, i.e. it does not depend on space at any instant of time.

The general flow equations for the various components present in block *i*, written in control volume finite difference terminology, may be presented as

$$\sum_{l\in\psi_i} T^m_{o_{l,i}}[(p^m_{o_l}-p^m_{o_i})-\gamma^m_{o_{l,i}}(Z_l-Z_i)]+\sum_{l\in\xi_i} q^m_{osc_{l,i}}+q^m_{osc_i}=\frac{V_{b_i}}{\alpha_c\Delta t}\{[\frac{\phi(S_o)}{B_o}]^{n+1}_i-[\frac{\phi(S_o)}{B_o}]^n_i\} \tag{F-a}$$

for the oil component, and

$$\sum_{l\in\psi_i} T^m_{w_{l,i}}[(p^m_{w_l}-p^m_{w_i})-\gamma^m_{w_{l,i}}(Z_l-Z_i)]+\sum_{l\in\xi_i} q^m_{wsc_{l,i}}+q^m_{wsc_i}=\frac{V_{b_i}}{\alpha_c\Delta t}\{(\frac{\phi S_w}{B_w})^{n+1}_i-(\frac{\phi S_w}{B_w})^n_i\} \tag{F-b}$$

for the water component.

where, ψ_i is a set whose elements are the existing neighboring blocks to block *i* in the core and ξ_i is a set whose elements are the core boundaries that are shared by block *i*. The primary unknowns are p_o and S_w, and the secondary unknowns are p_w and S_o, where $p_w = p_o - p_{cow}(S_w)$ and $S_o = 1 - S_w$.

The explicit, implicit, and Crank-Nicolson formulations have been derived from Equation F by specifying the approximation of time t^m as the first, second, and third integral approximation methods as referred to in Abukazem (2006)†. However, the explicit formulation is not used in multiphase flow because of time step limitations, and the Crank-Nicolson formulation is not commonly used.

In this study, some new assumptions have been added to the reservoir equations derived by Abukazem (2006). Fluid gravity effect is assumed to be negligible. Moreover, water and oil FVFs are considered to be equal to 1. Afterwards, the simplified equations have been applied for a one dimensional core with constant porosity. We coded IMPES (implicit-pressure-explicit-saturation) method to solve these equations.

Expanding the RHS of Equations F-a and F-b and rewriting them on the new assumptions, the following final equations are obtained:

† Petroleum Reservoir Simulations, J.H. Abou-Kassem S. M. Farouq-Ali M.R. Islam, 1st edition, Elsevier 2006, Gulf Publishing Company, ISBN: 978-0-9765113-6-6

$$\sum_{l\in\psi_n} T_{o_{l,n}}^{n+1}[(p_{o_l}^{n+1} - p_{o_n}^{n+1})] + \sum_{l\in\xi_n} q_{osc_{l,n}}^{n+1} + q_{osc}^{n+1} = -\frac{V_{b_n}\phi}{\alpha_c \Delta t}(S_{w_n}^{n+1} - S_{w_n}^{n}) \tag{G}$$

for the oil component, and

$$\sum_{l\in\psi_n} T_{w_{l,n}}^{n+1}[(p_{o_l}^{n+1} - p_{o_n}^{n+1}) - (p_{cow_l}^{n+1} - p_{cow_n}^{n+1})] + \sum_{l\in\xi_n} q_{wsc_{l,n}}^{n+1} + q_{wsc_{l,n}}^{n+1} = \frac{V_{b_n}\phi}{\alpha_c \Delta t}(S_{w_n}^{n+1} - S_{w_n}^{n}) \tag{H}$$

for the water component.

Applied IMPES method

The IMPES method, as mentioned above, leads to an implicit solution method for pressure followed by an explicit solution method for saturation. In the first step, the transmissibilites, capillary pressures, and coefficients of pressure difference in the well production rates are calculated explicitly. In each related boundary condition, water and oil equations may be combined to obtain the pressure equation for block *i* through the elimination of the saturation term $(S_{w_n}^{n+1} - S_{w_n}^{n})$ that appears on the RHS of equations. For the volumetric core (no-flow boundaries) subjected in this study, the final equations for oil pressure and water saturation may be written as:

$$\sum_{l\in\psi_n} (T_{o_{l,n}}^{n} + T_{w_{l,n}}^{n}) p_{o_l}^{n+1} - \sum_{l\in\psi_n} (T_{o_{l,n}}^{n} + T_{w_{l,n}}^{n}) p_{o_n}^{n+1} = \sum_{l\in\psi_n} T_{w_{l,n}}^{n} (p_{cow_l}^{n} - p_{cow_n}^{n}) - (q_{osc_n}^{n} - q_{wsc_n}^{n}) \tag{I}$$

which represents a tridiagonal matrix equation. The water saturation is then obtained from:

$$S_{w_n}^{n+1} = S_{w_n}^{n} + \frac{\alpha_c \Delta t}{V_{b_n}\phi}\{\sum_{l\in\psi_n} T_{w_{l,n}}^{n+1}[(p_{o_l}^{n+1} - p_{o_n}^{n+1}) - (p_{cow_l}^{n} - p_{cow_n}^{n})] + q_{wsc_n}^{n}\} \tag{J}$$

Validation

To validate this simulation model, it has been compared with the Buckley-Leverett method in a case (with the properties represented in Table A) assuming that capillary pressure is negligible like what is assumed in the Buckley-Leverett method. The results of the simulation model are shown in Figure B, and they show good agreement with the Buckley-Leverett's results.

Table A
Synthetic core and fluid properties.

Permeability (md)	100	**Entry Pressure (kPa)**	10
Area (cm^2)	9	λ	2
Length (cm)	60	K_{ro}^*	1
Porosity (fraction)	0.4	K_{rw}^*	1
Oil viscosity (cP)	0.1	n_o	3
Water viscosity (cP)	1	n_w	3

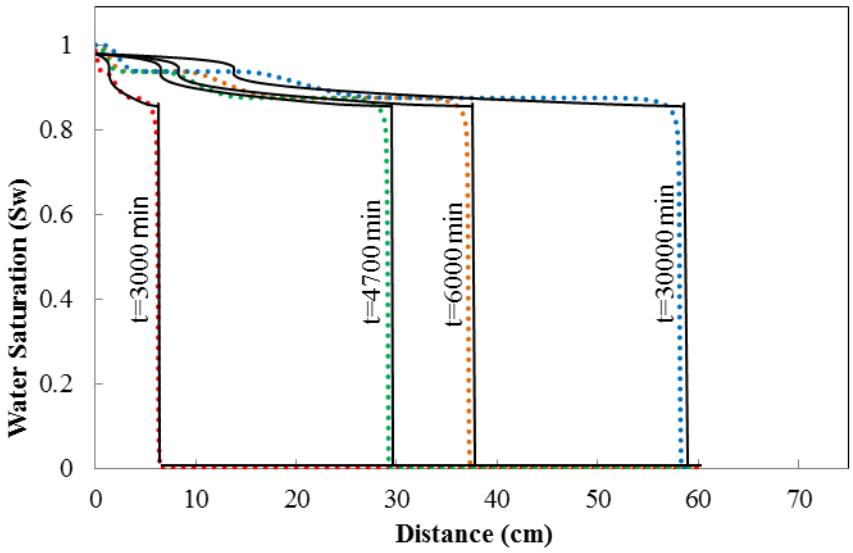

Figure B
Comparison of the simulator results with Buckley-Leverett results.